Challenges, Opportunities and Solutions in Structural Engineering and Construction – Ghafoori (ed.)
© 2010 Taylor & Francis Group, London, ISBN 978-0-415-56809-8

Experimental study of self-centering RC frames with column yielding mechanism

K. Sakino & H. Nakahara
Kyushu University, Fukuoka, Japan

ABSTRACT: This paper discusses the hysteresis behavior of a precast concrete structural system. The system is proposed based on innovative concepts for precast concrete frames using precast concrete units assembled by unbonded post-tensioned (PT) high strength steel bars. The precast concrete units are classified into three types according to their shapes. Each concrete unit is composed of one or two reinforced concrete beams and one or two plain concrete columns confined by steel tube. PT steel bars run through conduits embedded in the column of the precast concrete units. Each unit is connected to other unit with a connecting device and PT steel bars at a column-to-column joint at the mid-height portion of the columns in frames. After that, the reinforced concrete beams of the precast concrete units are connected by cast-in-sight concrete. The most significant characteristic of these unbonded PT precast concrete systems is their self-centering capability that results in essentially no residual drift after seismic events. The structural behavior under cyclic lateral load of a proposed precast concrete frame was examined by experimental study.

1 INTRODUCTION

In many reinforced concrete buildings, reinforced concrete frames and structural walls appear together. When lateral force resistance is provided by the combined contribution of frames and structural walls, it is customary to refer to them as a wall fame system, a dual system or a hybrid system. The Japanese term related to this type of system can be translated literally as wall frame system.

A goal in our research project is to establish a reliable performance-based seismic design (P-BSD) method for dual system buildings in which following abilities are required.

1. To control the largest story drift angle induced in the buildings during major earthquake ground motions (EQGMs) within limited value such as 0.01 rad
2. To control damages of non-structural elements as less as possible
3. To decrease permanent (residual) drift as small as possible
4. To avoid an expensive post-earthquake repair process
5. To afford large column-free spaces which could be easily remodeled
6. To be easily demolished when necessary

A proposed example of the prototype model for dual system buildings which might satisfy the demands described above is shown in Figure 1. The prototype building, which is so called double tube system, are composed of following structural elements.

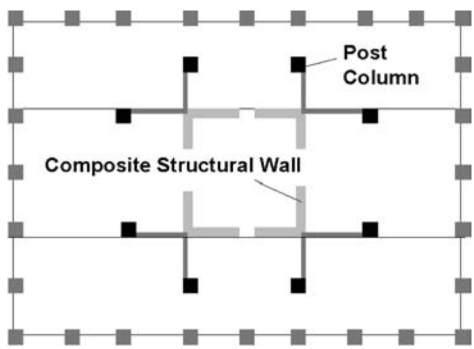

(a)

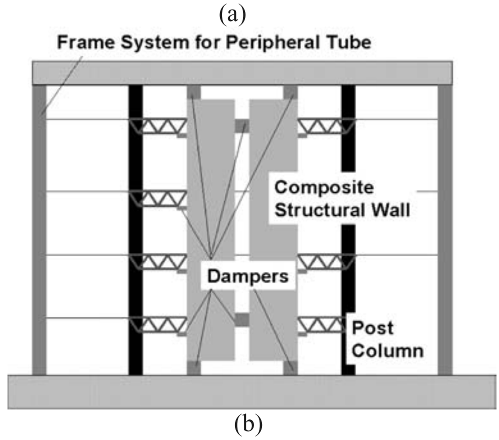

(b)

Figure 1. Prototype building: (a) plan; and (b) section.

Composite Structural Wall: The rolls of this element are to avoid weak story, to afford lateral stiffness and to behave as hysteretic dampers.

Frame System for Peripheral Tube: The roles of this frame system are to afford torsional rigidity of buildings, to sustain gravity load and to behave as a self-centering system which brings essentially no residual drift after EQGMs.

Truss Girder with Hysteretic Damper: The roles of this element are to afford an outrigger action to structural wall and to absorb earthquake energy by a bottom cord, which is attached to the structural wall, designed as hysteretic damper.

Post Column: The rolls of this element are to sustain gravity load and to resist overturning moment induced by earthquakes together with truss and structural wall.

An elastic-plastic behavior of the composite structural wall systems has been experimentally investigated and reported elsewhere (Sakino et al. 2004, Sakino & Hitaka 2006). The objectives of this paper are to propose a self-centering RC structural frame for the frame system for peripheral tube and to experimentally investigate a seismic performance of the new self-centering frame. The proposed self-centering frame system is different from a self-centering system proposed in the USA (Seo & Sause 2005) from the view points of a construction method and a collapse mechanism under lateral loading.

2 SELF-CENTERING FRAME SYSTEM

The frame system proposed in this paper is composed of precast concrete beam and column units assembled by using connecting devices and unbonded PT bars. The most significant characteristic of these unbonded PT precast concrete members is their self-centering capability that results in essentially no residual drift after EQGMs. The three-bay and two-story post-tensioned concrete frame system reported in this paper is shown in Figure 2. Figure 3 shows the deformed configuration of an unbonded post tensioned precast concrete beam and column sub-assemblage under lateral load due to EQGM. The behavior under lateral load is governed by the behavior of the interfaces between beams and columns which are fabricated monolithically. Opening of these interfaces at a selected level of lateral load provides a softening of the lateral load-drift behavior, in other words, a kind of hinges are formed at the top and bottom of the columns. Upon unloading, the post-tensioning force and the axial force due to gravity load tend to restore the structure to its original position (self-centering) by closing the gaps at the open interfaces. The characteristics and merits of the unbonded post-tensioned precast concrete frame system are itemized as follows.

1. Cracking in slab system and elongation of beams are not occurred, since the collapse mechanism of the frame is formed by openings of the interfaces between beams and columns as shown in Figure 3. This ensures a rigid-slab hypothesis.
2. As the position of the story in the frame is lower, the lateral load carrying capacity of the story increases due to the gravity load affect.
3. From the view point of a post-earthquake repair process, no hinging actions in beams are preferable.
4. On the other hand, the unbonded post-tensioned precast frame system has following defects.
5. An energy absorption capacity is hardly expected, because nonlinear behavior of the concrete in compression (refer to the deformed configuration shown in Figure 3) results in a narrow hysteresis loop.

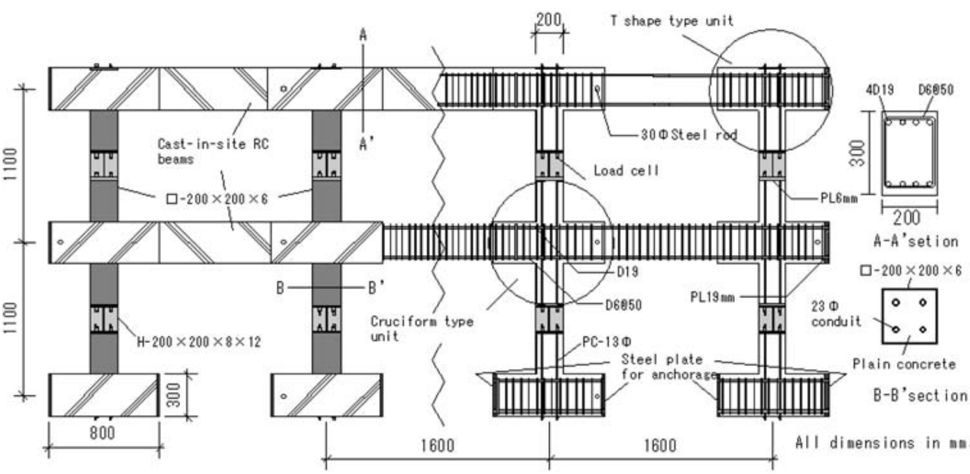

Figure 2. Self-centering frame system studied.

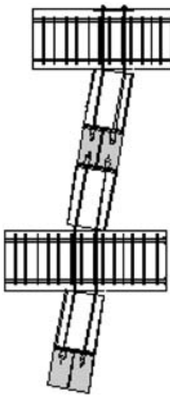

Figure 3. Schematic deformed configuration of unbonded PT precast column.

6. A story collapses mechanism, which should be avoided during EQGMs, could be introduced to the frame system.
7. Serious damages of column concrete could accompany opening of the interfaces between beams and columns.

These defects in the self-centering frame system can be overcome by introducing the composite structural walls with hysteretic dampers or by confining the column concrete by a steel tube which has a role of a formwork as well.

3 EXPERIMENTAL PROGRAMS

3.1 *Test specimen*

The matters of major interest in the experimental study were to examine feasibility of the construction method and the structural behavior of the proposed self-centering frame system. A specimen was three-bay, two-story model, and was scaled to 1/3 in order to utilize the available test facility. The dimensions and detailing of the specimen are shown in Figure 2, where an exterior view of the specimen is shown in left half, an arrangement of steel bars and PT bars is in right half. The sections of beams and columns are also shown in Figure 2. The specimen is composed of precast concrete units and column-to-column connecting devices. The precast concrete units are classified into two types according their shapes, i.e. T shape type and cruciform type. Each concrete unit is composed of two reinforced concrete beams and one or two plain concrete columns confined by square steel tube. A space of 10 mm width is provided between the beam surface and the steel tube which is used as a formwork for column concrete. Four conduits to thread the PT bars are embedded in each column. The column-to-column connecting device shown in Figure 4 is fabricated by using H shape steel so called as H-200 × 200 × 8 × 12 with stiffeners. These connecting devices were placed at the mid-height portions of the columns in frame. The eight connecting devices and the precast concrete units, which were eight T shape units and four cruciform units, were assembled by using PT bars at the site where the test was conducted. After that, the reinforced concrete beams of the precast concrete units are connected by cast-in-site RC beams. Eight deformed bars with nominal diameter of 19 mm (D19 bars) were used as longitudinal bars of beams, and D 6 bar hoops were placed at 50 mm space for transverse reinforcements. At the ends of three-span continuous beams, steel plates with 19 mm thickness were placed to be used as anchor devices for beam longitudinal bars which were welded to the steel plate. The fabrication of the frame specimen showed that the construction procedure described above was successfully verified to be feasible. The properties of steel materials are shown in Table 1. The cylinder strengths of concrete used for precast concrete units and cast-in-site concrete for connection RC beams were 38.4 MPa and 32.1 MPa, respectively.

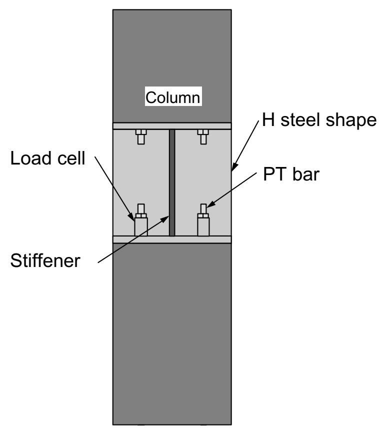

Figure 4. Column-to-column connecting device.

Table 1. The properties of steel materials.

Type of steel	σ_y (MPa)	σ_u (MPa)	Yong's modulus (GPa)	Elongation (%)
□ 200 × 200 × 6	397	474	205	34.3
D19 Steel bar	394	548	173	16.8
D6 Steel bar	333	503	177	15.1
H200 × 200 × 8 × 12	325	456	207	41.8
	306	464	204	37.3
13ϕ Post tensioned bar	1243	1288	192	11.0

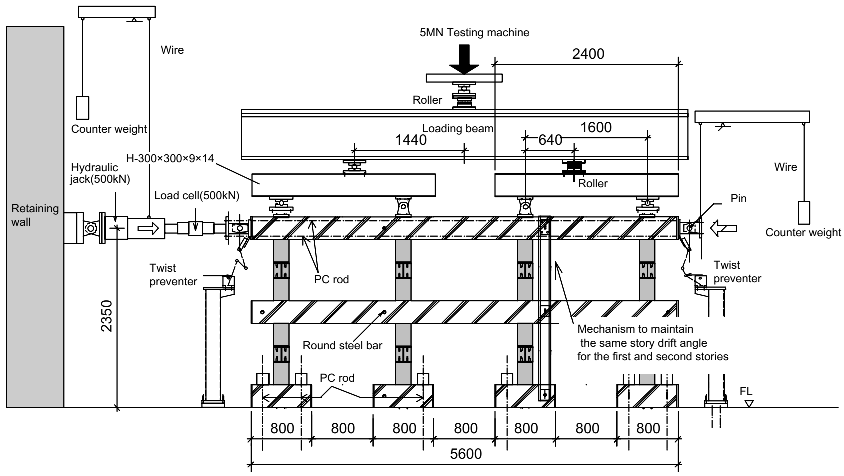

Figure 5. Loading set-up.

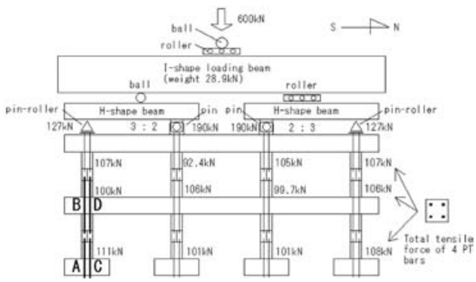

Figure 6. Axial force in each column.

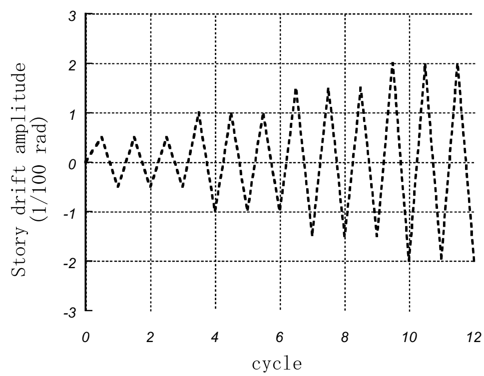

Figure 7. Loading program.

3.2 *Experimental apparatus and procedure*

A loading method is schematically shown in Figure 5. The vertical load corresponding to gravity load in the columns was applied at first to each column by using testing machine and three steel loading beams acting as vertical load distributor. The vertical load applied by testing machine was 600 kN and was kept constant during test. After applying the vertical load through testing machine, additional axial loads in columns were introduced by PT bars. The loads in PT bars were measured by specially made load cells shown in Figure 4. The axial load in each column introduced by testing machine, weight of loading beams and post tensioned bars is shown in Figure 6. The horizontal loads were applied to the specimen in a manner of pushing in both directions as shown in Figure 5, which introduced the compression axial force into the reinforce concrete beam. The loading pattern was a cyclic type with alternating drift reversals. The peak drifts were increased stepwise from 0.005 h, where h was the total height (2200 mm) of the two-story specimen, until 0.02 h with incremental drift of 0.005 h after three successive cycles at each drift level as shown in Figure 7. It is noteworthy that the story drift angles of the first and second story were kept to be the same during the test by the special mechanism attached to the specimen as shown in Figure 5.

4 EXPERIMENTAL RESULTS

4.1 *Load-deformation relationships*

Figure 8 shows a relation between the lateral load and story drift angle. The maximum lateral load at each amplitude increases, as the drift amplitude becomes larger. The larger drift amplitude results in larger opening at the interfaces between columns and beams as shown in Figure 3, hence larger forces in PT bars. This is verified by Figure 9 which shows a relation between story drift angle and total elongation of columns divided by total column height. The values of total elongation are taken as average values measured in four two-story columns. The increase of maximum lateral load can be attributed to an increase of axial loads in columns due to the increase of forces in PT bars. This phenomenon suggests that an introducing of larger initial forces in PT bars could bring larger lateral load capacity at relatively small story drift amplitude. As shown in Figure 8, the proposed frame system has the self-centering capability as expected. A detailed and quantitative estimation of self-centering capability is shown in Figure 10 which describes a relationship between story drift amplitude and residual story drift. As shown in Figure 10, the average residual story drift shown by dotted line can be estimated as small as 10% of the maximum story drift undergone. An observation of the specimen after the test revealed that there was substantially no damage in appearance.

Figure 11 shows relations between tension forces in four PT bars and story drift angles. The four PT bars are named as A, B, C, D, and they are referred as PT-A or PT-B and so on, hereafter. The places of these four PT bars are shown in Figure 6 under the same symbols A, B, C, D. As shown in Figure 6, PT-A and PT-C are placed in bottom half of left side column, and

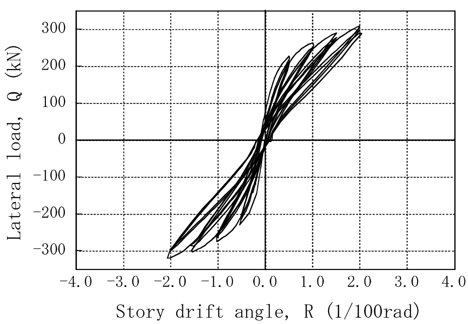

Figure 8. Experimental cyclic lateral load-drift behavior.

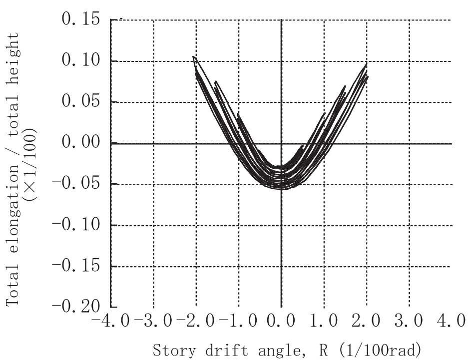

Figure 9. Relationship between axial elongation of columns and story drift.

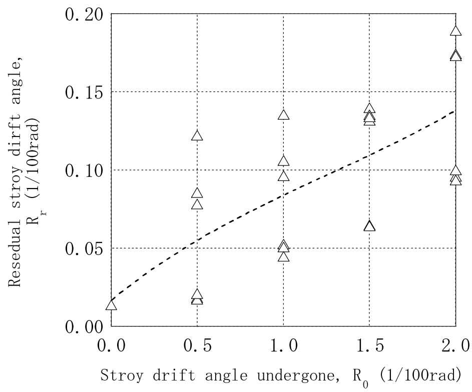

Figure 10. Relationship between residual story drift and story drift undergone.

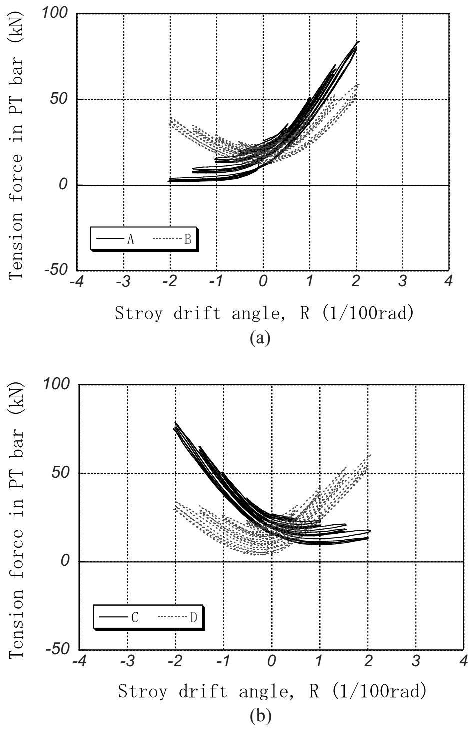

Figure 11. Tension force-drift behavior of PT bars: (a) PT-A, B; and (b) PT-C, D.

PT-B and PT-D are in middle part of the same column. The tension forces in PT-A and PT-C are shown by solid lines in Figures 11(a) and (b), and those in PT-B and PT-D are by dotted lines. As shown by solid lines in Figure 11, tension forces in PT bars in bottom half of the column are not fluctuated when they are placed in compression side due to bending moment, and are increased when in tension side. This means that resultant force of four PT bars in the bottom half (and/or top half) of the column has a bending moment component as well as tension force component. On the other hand, the dotted lines in Figure 11 show that tension forces in PT-B and PT-D behave in a similar manner. This means that resultant force of four PT bars in the middle part of the column has only axial-tension-force component. The hysteresis behavior of PT bars in the column described above is consistent with the deformed configuration of unbonded post tensioned precast concrete column shown in Figure 3.

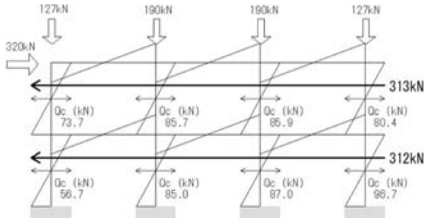

Figure 12. External load and internal force in the frame at the ultimate state.

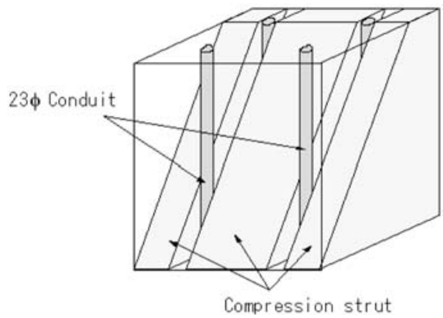

Figure 13. Ineffective width due to conduits.

4.2 *Ultimate lateral load capacity*

Figure 12 shows external vertical and lateral loads applied by loading system and shearing forces in columns at the loading point when the story drift reached the largest value of 0.02 h at first. The lateral load of 320 kN is the maximum lateral load measured in this test. The shearing force, Q_c, of each column is a value calculated from the bending moment capacities, M_c, at the top and bottom of each column. The bending moment of columns is obtained by Equation (1).

$$M_c = {}_sM + {}_cM$$
$${}_cM = \frac{N_m}{2}\left({}_cD - \frac{N_m}{{}_c\sigma_{cB}\cdot{}_cb}\right) \qquad (1)$$

where, ${}_sM$ is a bending moment component of four PT bars in the column, ${}_cM$ is a ultimate moment capacity of plain concrete section of the column under an axial force N_m, ${}_c\sigma_B$ is a compressive strength of concrete confined by square steel tube (Sakino & Sun 1994), ${}_cD$ is a depth of concrete column section and ${}_cb$ is an effective width of concrete column section which is defined by neglecting an ineffective width due to the conduits as shown in Figure 13. It is noteworthy that the axial force Nm is calculated by considering shearing forces in the beams and a tension axial force component of the resultant force of the four PT bars in the column measured by load cells. As shown in Figure 12, the calculated lateral load capacities of the first and second stories, which are 312 kN and 313 kN, respectively, are almost same as the experimental lateral load capacity of 320 kN.

5 CONCLUSIONS

The following conclusions are reached on bases of the experimental study on the self-centering RC structural frame compose of precast concrete units, column-to-column connecting devices and unbonded post tensioned bars.

1. It is verified to easily fabricate the three-bay, two-story self-centering frame by construction procedure proposed in this paper.
2. The hysteresis behavior of the frame under cyclic lateral loading was stable, and showed self-centering capability.
3. The value of maximum residual story drift angle was less than 0.002 rad as expected.
4. The lateral load capacity of the frame specimen can be predicted with a very reasonable accuracy by the calculation method used in this paper.

REFERENCES

Sakino, K. & Sun. Y. 1994. Stress-strain curve of concrete confined by rectilinear hoop. Journal. Structural and Construction, Engineering. AIJ, 461, 95–104.

Sakino, K. et al. 2004. Cyclic test on composite wall-frame subassmblage. 13th World conference on earthquake engineering, Vancouver, B.C., Canada, August 1–6, 2004 Paper No. 3172.

Sakino, K. & Hitaka, T. 2006. Experimental study on overturning moment-resisting structural walls with steel hysteretic dampers. Prod. of 8th National conference of earthquake engineering, DVD-ROM, 2006, April 18–23.

Seo, C.Y. & Sause, R. 2005. Ductility demands on self-centering systems under earthquake loading. ACI Structural Journal, Title No. 102-S28, pp. 275–285, March–April 2005.